Dual-Frequency Generation in the L Band by a Gyromagnetic Nonlinear Transmission Line (GNLTL)

J.J. Barroso[1], J.O. Rossi[1], F.S. Yamasaki[1], J.P. Leite Neto[1],E. Schamiloglu[2]

[1]National Institute for Space Research (INPE), Sao José dos Campos and [2]University of New Mexico (UNM), Albuquerque, USA

Abstract — Gyromagnetic nonlinear transmission lines (GNLTLs) are a type of non-dispersive coaxial transmission line loaded with ferrite on the inner conductor that can generate high-power microwave RF signals and sharpen high-voltage pulses. GNLTLs are advantageous for compact high-power microwave sources due to their solid-state nature, thus circumventing the need for vacuum tubes or gas switches, and they find applications in radar, electronic warfare, and pulsed power systems. Through numerical simulation, the present work demonstrates the capability of GNLTLs in generating two output oscillatory RF pulses from a single input voltage pulse. This is achieved by properly adjusting both the flattop time of the input pulse and the output load of the line. We show the generation of a dual-frequency RF pulse with two frequencies (1.75 and 1.57 GHz) in a single signal. The frequencies lie in the L-band, which is widely used in telecommunications and navigation, as their longer wavelengths can easily penetrate clouds, rain, and tree foliage with minimal signal loss.

I. INTRODUCTION

High-Power Microwave (HPM) systems, usually characterized by powers ranging from kilowatt to multi-gigawatt levels during peak operations, have transitioned from physics experiments to essential components of defense and electronic warfare, industrial material processing and synthesis, frontier scientific research, next-generation communications, and deep-space radar. Dating back to the 1990s, Gyromagnetic Nonlinear Transmission Lines (GNLTLs) have represented a paradigm shift in high-power microwave (HPM) generation [1]. While traditional sources rely on the interaction between an electron beam and a vacuum slow-wave structure, GNLTLs operate on solid-state, electromagnetic wave propagation principles within a transmission line. Traditional HPM sources are vacuum-tube devices that require a high-energy electron beam to be generated, focused, and modulated (klystrons, TWTs, gyrotrons). In contrast, a GNLTL is a completely solid-state/coaxial system, relying on the nonlinear magnetic permeability of ferrimagnetic materials (like NiZn or MgMn ferrites), and requires no vacuum pumps or electron beams, drastically reducing weight and volume. GNLTLs consist of structures loaded with ferrite beads that exploit gyromagnetic precession for applications such as pulse sharpening [2], high-power microwave generation [3], and magnetic pulse compression combining three functions in one device. GNLTLs have successfully consolidated specialized segments where compactness, ruggedness, and frequency agility are more crucial than gigawatt power or continuous-wave operation, evolving from laboratory novelties into viable replacements for traditional sources on four major technological fronts: tactical counter-unmanned aircraft systems (C-UAS) and compact HPM [4]; frequency agility and electronic warfare and phased arrays via coherent multichannel summation [5]; and aerospace and satellite disruptors [6].

The present work demonstrates the previously unexplored capability of GNLTLs in generating two output oscillatory RF pulses from a single input voltage pulse. This is achieved by properly adjusting both the flattop time of the input pulse and the output load of the line. The line considered here to exploit the proposed approach is a 6-12 kV-driven GNLTL developed by our group [1]. The study shows here that a GNLTL can operate simultaneously in/at two different output frequencies (1.75 GHz and 1.57 GHz) operate in the L band (1-2 GHz), where the two oscillatory output pulses superimpose the primary excitation pulse.

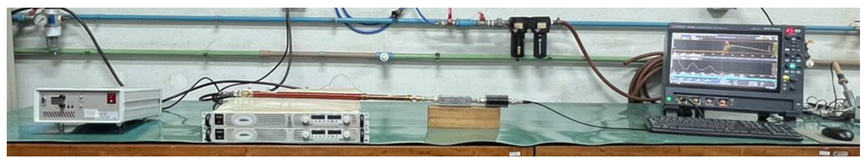


Fig. 1 GNLTL experimental setup

II. GNLTL DESCRIPTION AND OPERATION PRINCIPLE

A GNLTL is typically a coaxial transmission line loaded with ferrimagnetic material (usually NiZn ferrite) on the inner conductor. A magnetic biasing field is externally applied along the transmission line's central axis inside the material to initially align the magnetic moments within the ferrite material in the longitudinal direction (Fig. 1). RF Generation: The nonlinear precession of the magnetic moments induces high-frequency oscillations in the propagating pulse along the line. Such oscillations convert the input pulse into a train of RF oscillations, which are emitted as the output signal, with frequencies varying from hundreds of MHz to a few GHz.

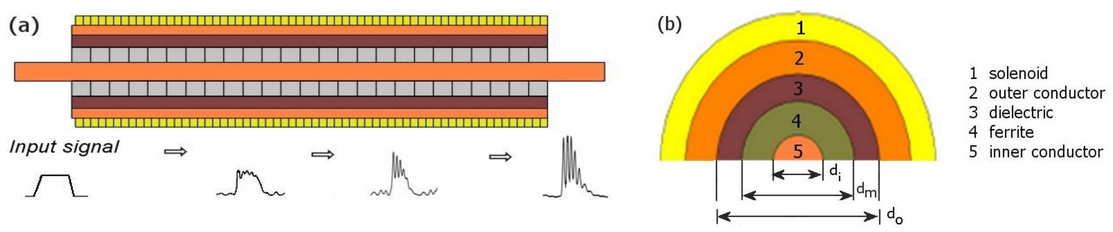


Fig. 2 (a) GNLTL schematic with its elements, illustrating the formation of a train of solitons in the line output. (b) Cross sectional view, where d_i and d_m are the inner and outer diameters of the ferrite ring; d_0 is the inner diameter of the outer conductor.

III. GNLTL MODELING

Two processes occur simultaneously in the generation of microwave oscillations. The precession of the magnetization vector M and the interaction of M with the TEM-mode wave propagating through the coaxial line. Both processes can be described by two linearly coupled circuit equations that model voltage and current along the two-conductor transmission line [2], as given below by (1). In (1), I is the current, V the voltage, and C_0 and L_0 are linear capacitance and inductance per unit length; ϕ_m is the circumferential flux linkage (per unit length) coupling the inner and outer coaxial conductors, described by (2), where M_ϕ is the circumferential magnetization. In finite-difference form, the electric circuit and magnetization equations, (1) and (2), are represented by a lumped-parameter network in Fig. 3.

$$dI/dz = C_0\ dV/dt\ ;\ dV/dz = L_0\ dI/dt + d\phi_m/dt \quad (1) \qquad \phi_m = \int_{d_i/2}^{d_m/2} \mu_0 M_\phi(r)dr = \mu_0\left(\frac{d_m - d_i}{2}\right)M_\phi \quad (2)$$

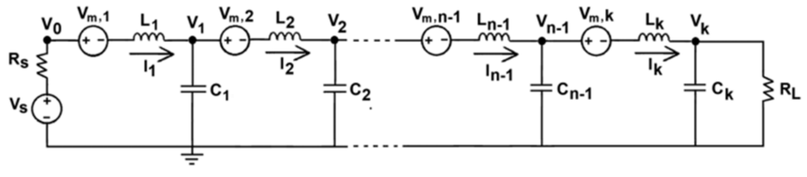


Fig. 3. Network circuit representing a gyromagnetic transmission line (GNLTL), where the state variables are $\{I_k, V_k, M_k\}$, namely, current I_k through the inductor of section k, voltage V_k across the capacitor C_k, and the voltage source $V_{m,k}$ induced by magnetization M_k.

The circuit and flux linkage equations (1) and (2) are solved jointly with the Landau-Lifshitz-Gilbert (LLG) equation that describes the GNLTL magnetization dynamics. Upon discretizing the distributed gyromagnetic line (Fig. 2) in capacitive and inductive lumped elements, we arrive at a system of first-order differential equations, with state variables {I, V, Mr, $M\phi$, Mz} which is numerically solved by using adaptive methods based on explicit Runge-Kutta and and implicit methods [2].

IV. RESULTS AND DISCUSSION

Figure 4(a) displays the simulated output voltage pulse for a 7 kV-amplitude trapezoidal input pulse with rise, flattop, and fall times, respectively, of {4, 3, 4} ns. Small RF oscillations on the upper portion of the output show that the GNLTL acts as a pulse sharpener, producing a compressed output pulse with a rise time of ~1ns. However, when the input pulse rise time is reduced to 2 ns (Fig. 4(b)), the GNLTL operates as an RF generator, resulting in the production of strong oscillations with a modulation index of 47 %. Based on the time interval between consecutive pulses, we infer a generated frequency of 2.2 GHz. Besides the dissimilar amplitudes of the RF oscillations in Figs. 4(a) and 4(b), additional features are noticeable. The output pulse in Fig. 4(b) contains an oscillatory tail caused by load reflection. Six crests appear, extending from 15 to 25 ns, which matches with the number of peaks following the leading edge (~6ns) of the oscillatory burst. Extending the flattop duration to 5 ns (Fig. 5(a)), an isolated bump appears around 13 ns. Increasing further the input pulse flattop to 12 ns (Fig. 5(b)) yields two oscillating bursts, with the RF train (originating from the reflected pulses) having a DC value close to 7 kV. The high-pass filtered RF bursts with the DC components removed are displayed in Fig. 6, and their corresponding frequency spectra are shown in Fig. 7. The oscillatory train produced by the nonlinear gyromagnetic mechanism features a center frequency of 1.75 GHz, whereas the spectrum of the RF train formed by load reflection exhibits a comparable frequency of 1.57 GHz.

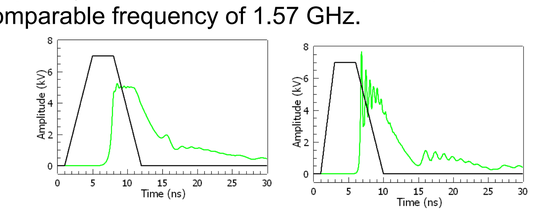


Fig. 4. (a) Output pulse (green line) from a 7-kV amplitude trapezoidal input pulse with rise, flattop, and fall times of {4, 3, 4} ns respectively. (b) The same as in (a) but with {2, 3, 4}. The output load, R_L, is made equal to the line characteristic impedance Z_0=73.0 Ω.

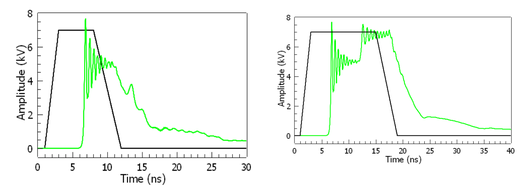


Fig. 5. (a)The same as in Fig. 4 but with input pulse of rise, flattop, and fall times of {2, 5, 4} ns respectively. (b) The same as in (a) but rise, flattop, and fall times of {2, 12, 4}, respectively.

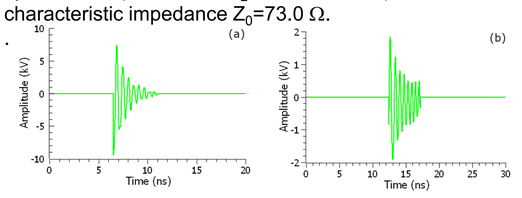


Fig. 6. High-pass filtered time signals in Fig. 4(b) with DC components removed.

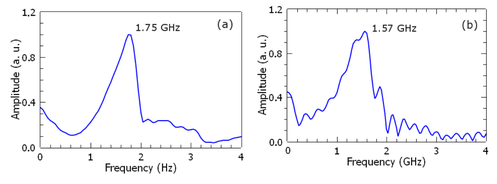


Fig. 7. Frequency spectra of the time signals in Fig. 5.

In concluding this section, we examine the effect of the resistive load R_L on the buildup of the lower frequency oscillatory waveform due to input pulse reflection at the end of the GNLTL. In the previous cases (Figs. 4 and 5), R_L was set at the line characteristic impedance Z_0. Now making R_L=0.8 Z_0 and decreasing the flattop time to 10 ns leads to an output (see Fig. 8) similar to that in Fig. 5 (b). But this case shows additional features of the two RF output pulses. The higher-frequency (1.82 GHz) RF pulse on the left side of Fig. 8 contains non-sinusoidal distortions related to the nonlinear gyromagnetic dynamics and to the high-voltage shockwave propagation through the magnetically biased ferrite. However, the lower frequency (1.69 GHz) pulse on the right consists of a train of sinusoidal pulses that originate from pulse reflection.

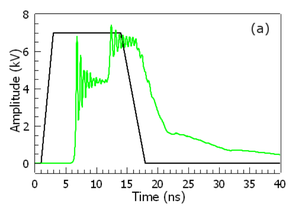


Fig. 8. Output pulse (green line) from a 7-kV amplitude trapezoidal input pulse with rise, flattop, and fall times of {2, 10, 4} ns, respectively. In this case, R_L=0.8 Z_0.

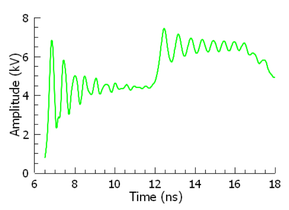


Fig. 9. A zoomed-in view of the RF pulses of Fig. 8. The oscillation frequencies of the left side and the right one are 1.82 GHz and 1.69 GHz, respectively.

Fig. 9 shows a zoomed-in view of the RF pulses in Fig. 8. The incident pulse reflects at the end of the line, while the reflected one travels in the opposite direction (backward). These two pulses superimpose on the trailing edge of the forward pulse, such that the forward and backward pulses add together at every point along the line. Because the reflected energy is delayed, it acts as a secondary overlapping pulse, smoothing and rounding the sharp and abrupt corners of the reflected RF pulse.

V. CONCLUSIONS

Relying on numerical simulations, the present work has presented a dual-frequency microwave source (two distinct RF oscillations at 1.75 and 1.57 GHz) based on a small-scale GNLTL. As a further functionality of GNLTLs, these frequencies can be tuned by changing either the axial biasing magnetic field or the input pulse voltage amplitude. Currently, the generation techniques for dual-frequency microwave pulses are realized by active mode-locked optoelectronic oscillators (AML-OEOs) or similar photonic devices combined with pulse modulation or shaping. A key component of such devices is a dual-drive Mach-Zehnder modulator, which allows independent or combined modulation on two RF ports, enabling nonlinear mixing and dual-tone generation. Nevertheless, the compact L-band tunable source proposed here is a simpler device that offers excellent prospects in multi-band radar, communications, electronic warfare, and remote sensing thanks to its agile dual-frequency capability.

REFERENCES

1. V. P. Gubanov et al., Tech. Phys. Let.t, vol. 35(7), 2009.
2. A. F. Greco, et al., Rev. Sci. Instrum. 93, 065101, 2022.
3. P. V. Priputnev al., Tech. Phys., vol. 68(5), 2023.
4. J. O. Rossi et al., Rev. Sci. Instrum. 93, 024704, 2022.
5. W. Hendricks et al., IEEE Trans. Plasma Sci., 4(3), 2026.
6. www.metamag.us/products/non-linear-transmission-lines